Progress in Fractional Differentiation and Applications
An International Journal

http://dx.doi.org/10.18576/pfda/050204

On Comparison of Two Reliable Techniques for the Riesz Fractional Complex Ginzburg- Landau-Schrödinger Equation in Modelling Superconductivity

*Asim Patra**

Department of Mathematics National Institute of Technology Rourkela, Odisha, India

Received: 2 Aug. 2018, Revised: 2 Nov. 2018, Accepted: 11 Nov. 2018
Published online: 1 Apr. 2019

Abstract: In the present paper, the Complex Ginzburg-Landau-Schrödinger (CGLS) equation with the Riesz fractional derivative has been treated by a reliable implicit finite difference method (IFDM) of second order. Furthermore for the purpose of a comparative study and for the investigation of the accuracy of the resulting solutions, another effective spectral technique viz. time-splitting Fourier spectral (TSFS) technique has been utilized. In case of the finite difference discretization, the Riesz fractional derivative is approximated by the fractional centered difference approach. Further the stability of the proposed methods has been analysed thoroughly and the TSFS technique is proved to be unconditionally stable. Moreover the absolute errors, for $|\Psi(x,t)|^2$ obtained from both the techniques for various fractional orders, have been tabulated. Further the L^2 and L^∞ error norms have been displayed for $|\Psi(x,t)|^2$ and the results are also graphically depicted.

Keywords: Complex Ginzburg-Landau-Schrödinger (CGLS) equation, Riesz fractional derivative, fractional centered difference, time-splitting Fourier spectral method.

1 Introduction

The concept of fractional differential equations is very old but in the recent years it has shown tremendous growth of interest among the researchers. The field of fractional calculus plays a very significant role in modelling various anomalous transport phenomena. There are several applications of the fractional differential equations in areas like engineering, physics, astrophysics, chemistry, control theory, dynamics of complex systems, fluid dynamics, other sciences and historical summaries for the growth and advancement of fractional calculus [1,2,3,4]. The concept of Riesz derivative can be explained as the mathematical combination of the left and right Riemann-Liouville derivatives for which it is used in several real life phenomena. Technically, the Riesz derivative has become a very important tool to be utilized in the fractional modelling owing to its nonlocal and dual nature. Moreover the idea of Riesz derivative is generally used in several equations which describe the applications in random walk models and anomalous diffusion characterized by nonlinear dependence of the mean square displacement of a diffusing particle over time.

The present paper deals with the Riesz fractional Complex Ginzburg-Landau-Schrödinger(CGLS) equation

$$(\eta - i\beta)\frac{\partial \psi}{\partial t} = \frac{\partial^\alpha \psi}{\partial |x|^\alpha} + \frac{1}{\varepsilon^2}(V(x) - |\psi|^2)\psi, \ \ x \in \Re, \ \ t > 0, \tag{1}$$

with initial condition

$$\psi(x,0) = \psi_0(x), \ \ x \in \Re. \tag{2}$$

* Corresponding author e-mail: asimp1993@gmail.com

where $\psi(x,t)$ is a complex wave function and $\frac{\partial^{\alpha}\psi}{\partial|x|^{\alpha}}$, denoting the Riesz derivative with fractional order α, can also be represented by $\frac{\partial^{\alpha}\psi}{\partial|x|^{\alpha}} = -(-\triangle)^{\alpha/2}\psi(x,t)$. Here η and β are two nonnegative constants satisfying $\eta+\beta>0$, $\beta\neq 0$ in the complex case and the real-valued external potential $V(x)$ takes the form

$$V(x) = \frac{1}{1+exp(-\gamma_x x^2)}, \tag{3}$$

where γ_x is a positive constant. Moreover ε is a positive constant which takes the value unity in the standard CGLS equation but $0<\varepsilon<1$ for the CGLS equation in the semi-classical regime. Here the complex order parameter case is taken into consideration which defines the modelling of superconductivity process.

The Complex Ginzburg-Landau-Schrödinger (CGLS) equation is a nonlinear equation that describes a variety of phenomena from the second-order phase transitions to superconductivity and Bose-Einstein condensation to liquid crystals and strings in the field theory. Further, the spectral methods have emerged as a viable technique for solving the partial differential equations because of its high accuracy. Moreover there have been only a few studies of applicability of spectral methods to the fractional CGLS equation. Motivated by this knowledge, the Riesz fractional Complex Ginzburg-Landau-Schrödinger (CGLS) equation in this article, has been treated by an effective scheme known as the time-splitting Fourier spectral method which can be otherwise described as a scheme of finding the solution in smaller steps. This technique is actually very efficient and powerful in handling the non-linear partial differential equations [5,6,7]. In addition to that an implicit finite difference method (IFDM) has been used for solving the Riesz fractional partial differential equation where the Riesz fractional derivative is approximated by the fractional centered difference scheme.

The numerical techniques and methodologies for tackling the Riesz fractional complex Ginzburg-Landau-Schrödinger equation is limited in the literature to certain extent. Therefore, the techniques represented in the paper would prove to be highly desirable and effective. First of all, the implicit finite difference discretization technique involved by Celik et al [8] for the Riesz fractional diffusion equation is included here.

Lin et al [9] have depicted the dynamics, pinning and hyteresis of Ginzburg-Landau equation. Further Zhang et al [10] have studied the vortex dynamics in the Ginzburg-Landau- Schrödinger equation via numerical approach. In a different article, Patra [11] have studied regarding the spectral solutions of the Schrödinger equation. Further Aderogba et al [12] considered the fractional step splitting technique for the Cahn-Hilliard equation and discussed numerical results. The heat equation has been treated numerically via the spectral method by Thapa et al[13]. Saha Ray [14] had tackled the coupled Klein-Gordon-Schrödinger equations by means of the splitting spectral method. Furthermore Thalhammer et al[15] dealt with the higher order time-splitting Hermite and Fourier spectral methods. Jian et al [16] have presented the vortex dynamics in the Ginzburg-Landau equation in the inhomogeneous superconductors. The time splitting spectral scheme has been further studied by Bai and Wang [17] for the Schrödinger-Boussinesq equations. In another article, the quadratic observables of Schrödinger type equations have been numerically approximated by Markowich et al[18]. Wang [19] utilized the time splitting spectral method for the coupled Gross Pitaevskii equations.

The organization of this research article is done in the following manner: firstly, certain basic preliminaries for the Riesz fractional derivative and discrete Fourier transform have been specified in section 2. Then, section 3 comprises of the description of the numerical IFDM for the Riesz fractional CGLS equation. Then the stability has been analysed for the proposed implicit numerical method in section 4 via von Neumann stability analysis. In section 5, an effective fourier spectral approach is exhibited for the proposed fractional equation via splitting technique. Then in section 6, the splitting scheme is proved to be unconditionally stable. Furthermore section 7 displays the tabulated results along with the numerical explanation regarding various solutions of absolute value of the complex wave function. Furthermore, this section also depicts the graphical solutions. Then finally the conclusion is included in section 8.

2 Basic preliminaries of fractional calculus

In this section some primary concepts regarding the Riesz derivative have been discussed. Moreover some of the formulae, which will be later used, regarding the discrete Fourier transform and inverse discrete Fourier transform have been displayed.

Definition 1: For a fractional order $\alpha(n-1<\alpha\leq n)$, the Riesz derivative, for the domain $-\infty<x<\infty$, is defined as [11]

$$\frac{\partial^{\alpha}\psi(x)}{\partial|x|^{\alpha}}=-c_{\alpha}({}_{-\infty}D_{x}^{\alpha}\psi(x)+{}_{x}D_{\infty}^{\alpha}\psi(x)), \tag{4}$$

where ${}_{-\infty}D_{x}^{\alpha}\psi(x)$ is the Riemann-Liouville left derivative defined as

$${}_{-\infty}D_{x}^{\alpha}\psi(x)=\frac{1}{\Gamma(n-\alpha)}\frac{\partial^{n}}{\partial x^{n}}\int_{-\infty}^{x}\frac{\psi(\xi)d\xi}{(x-\xi)^{1-n+\alpha}} \tag{5}$$

and ${}_{x}D_{\infty}^{\alpha}\psi(x)$ is the Riemann-Liouville right derivative defined as

$${}_{x}D_{\infty}^{\alpha}\psi(x)=\frac{(-1)^{n}}{\Gamma(n-\alpha)}\frac{\partial^{n}}{\partial x^{n}}\int_{x}^{\infty}\frac{\psi(\xi)d\xi}{(\xi-x)^{1-n+\alpha}} \tag{6}$$

and

$$c_{\alpha}=\frac{1}{2cos\frac{\alpha\pi}{2}},\quad \alpha\neq 1. \tag{7}$$

When $\alpha=1$, we have

$$D_{x}^{1}\psi(x)=\frac{d}{dx}H\psi(x)=\frac{d}{dx}\frac{1}{\pi}\int_{-\infty}^{\infty}\frac{\psi(z)dz}{z-x}, \tag{8}$$

where the integral is considered in the Cauchy principal value sense and H denotes the Hilbert transform of $\psi(x)$.

If we consider a function $\psi(x,t)$ in particular which satisfies the boundary conditions $\psi(a,t)=\psi(b,t)=0$, which can be extended by taking $\psi(x,t)\equiv 0$ for $x\leq 0$ and $x\geq b$. Now, the Riesz fractional derivative of order $\alpha(n-1<\alpha\leq n)$ can be defined for $\psi(x,t)$ on the finite interval $a\leq x\leq b$

$$\frac{\partial^{\alpha}\psi(x,t)}{\partial|x|^{\alpha}}=-\frac{1}{2cos\frac{\alpha\pi}{2}}({}_{-\infty}D_{x}^{\alpha}\psi(x,t)+{}_{x}D_{\infty}^{\alpha}\psi(x,t)), \tag{9}$$

where

$${}_{-\infty}D_{x}^{\alpha}\psi(x,t)=\frac{1}{\Gamma(n-\alpha)}\frac{\partial^{n}}{\partial x^{n}}\int_{a}^{x}\frac{\psi(\xi,t)d\xi}{(x-\xi)^{1-n+\alpha}}, \tag{10}$$

and

$${}_{x}D_{\infty}^{\alpha}\psi(x,t)=\frac{(-1)^{n}}{\Gamma(n-\alpha)}\frac{\partial^{n}}{\partial x^{n}}\int_{x}^{b}\frac{\psi(\xi,t)d\xi}{(\xi-x)^{1-n+\alpha}}. \tag{11}$$

Definition 2: Now for solving the equation in the later section of the paper, certain definitions for the discrete Fourier transformations are presented here. The discrete Fourier transformation of ψ_j is defined from $t=t_n$ to t_{n+1} as

$$\psi_{k}(t)=F_{k}[\psi_{j}(t)]=\sum_{j=0}^{m-1}\psi(t)exp(-i\mu_{k}(x_{j}-a)),\ \ k=-\frac{m}{2},\cdots\frac{m}{2}-1, \tag{12}$$

where $\mu_k=\frac{2\pi k}{b-a}$ is the transform parameter and the domain of x is $[a,b]$.

Similarly the inverse discrete Fourier transformation is given by

$$\psi_{j}(t)=F_{j}^{-1}[\psi_{k}(t)]=\frac{1}{m}\sum_{k=-\frac{m}{2}}^{\frac{m}{2}-1}\psi_{k}(t)exp(i\mu_{k}(x_{j}-a)),j=0,1,2,\cdots,m-1. \tag{13}$$

3 Second-order implicit finite difference method for the fractional complex Ginzburg-Landau- Schrödinger equation with the Riesz fractional derivative

In this section an implicit second-order finite difference technique has been utilized to deal with the following Riesz fractional Complex Ginzburg-Landau-Schrödinger equation

$$(\eta - i\beta)\frac{\partial \psi(x,t)}{\partial t} = \frac{\partial^{\alpha}\psi(x,t)}{\partial |x|^{\alpha}} + \frac{1}{\varepsilon^2}(V(x) - |\psi(x,t)|^2)\psi(x,t), \;\; x \in \Re, \;\; t > 0, \tag{14}$$

with initial condition

$$\psi(x,0) = \psi_0(x), \;\; x \in \Re, \tag{15}$$

where $\psi(x,t)$ is a complex valued wave function.

Lemma 3.1: Let $f \in C^5(\Re)$ with the assumption that the derivatives up to order less than or equals to five belong to the $L_1(\Re)$ space. Further let the fractional centered difference be given by

$$\triangle_h^{\alpha} f(x) = \sum_{-\infty}^{\infty} \frac{(-1)^j \Gamma(\alpha+1)}{\Gamma(\frac{\alpha}{2} - j + 1)\Gamma(\frac{\alpha}{2} + j + 1)}. \tag{16}$$

This renders us with

$$-\frac{1}{h^{\alpha}} \triangle_h^{\alpha} = \frac{\partial^{\alpha} f(x)}{\partial |x|^{\alpha}} + O(h^2). \tag{17}$$

From Eq. (17) it can be assured that when $h \to 0$, the term $\frac{\partial^{\alpha} f(x)}{\partial |x|^{\alpha}}$ represents the Riesz fractional derivative of order α for $1 < \alpha \leq 2$. Proof: Regarding the proof of the lemma, the reader can refer [8].

Corollary 1.: *An efficient result has been derived by Celik et al[8] stating that if $f^*(x)$ is defined by*

$$f^*(x) = \begin{cases} f(x), & x \in [a,b] \\ 0, & x \notin [a,b] \end{cases} \tag{18}$$

provided $f^* \in C^5(\Re)$ and the derivatives of $f^*(x)$ upto order five belongs to the $L_1(\Re)$ space, then for the Riesz derivative of fractional order $\alpha(1 < \alpha \leq 2)$

$$\frac{\partial^{\alpha} f(x)}{\partial |x|^{\alpha}} = \frac{(-1)^j \Gamma(\alpha+1)}{\Gamma(\frac{\alpha}{2} - j + 1)\Gamma(\frac{\alpha}{2} + j + 1)} \tag{19}$$

where $h = (\frac{b-a}{m})$, and m is the number of partitions of the interval $[a,b]$.

Now the implicit second-order finite difference discretization scheme for Eq. (14) is given by

$$(\eta - i\beta)(\frac{\psi_i^{n+1}}{\tau}) - \frac{1}{2}(-h^{-\alpha})(\sum_{j=i-m}^{i} g_j \psi_{i-j}^{n+1} + \sum_{j=i-m}^{i} g_j \psi_{i-j}^{n}) =$$

$$\frac{1}{\varepsilon^2}(V(x)(\frac{\psi_i^{n+1}}{2} + \psi_i^n) - \frac{1}{2}((\psi_i^{n+1})^2 \overline{\psi}_i^{n+1} + (\psi_i^n)^2 \overline{\psi}_i^n)) + R_i^{n+\frac{1}{2}}, \tag{20}$$

where $R_i^{n+\frac{1}{2}}$ is the local truncation error.

4 Stability analysis via Von Neumann for the implicit finite difference method

Theorem 4.1: The implicit finite difference scheme in Eq. (20) is unconditionally stable.
Proof: The implicit scheme is given by

$$\psi_i^{n+1} = \psi_i^n - \frac{\tau}{2(\eta - \sqrt{-1}\beta)} h^{-\alpha} \sum_{j=i-m}^{i} g_j \psi_{i-j}^{n+1} - \frac{\tau}{2(\eta - \sqrt{-1}\beta)} h^{-\alpha} \sum_{j=i-m}^{i} g_j \psi_{i-j}^{n} +$$

$$\frac{\tau}{(\eta-\sqrt{-1}\beta)\varepsilon^2}(V(x)(\frac{\psi_i^{n+1}+\psi_i^n}{2})-\frac{1}{2}((\psi_i^{n+1})^2\overline{\psi}_i^{n+1}+(\psi_i^n)^2\overline{\psi}_i^n)), \tag{21}$$

where $\beta \neq 0$.

Let $\psi_i^n = \xi^n e^{\sqrt{-1}\omega ih}$, with $\xi > 0$. Then, we obtain

$$\xi^{n+1}e^{\sqrt{-1}\omega ih} = \xi^n e^{\sqrt{-1}\omega ih} - \frac{\tau}{h^\alpha(\eta-\sqrt{-1}\beta)}\frac{1}{2}(\sum_{j=i-m}^{i} g_j\xi^{n+1}e^{\sqrt{-1}\omega(i-j)h}+\frac{1}{2}(\sum_{j=i-m}^{i} g_j\xi^n e^{\sqrt{-1}\omega(i-j)h})+$$

$$\frac{\tau}{2(\eta-\sqrt{-1}\beta)\varepsilon^2}(V(x)(\xi^{n+1}e^{\sqrt{-1}\omega ih}+\xi^n e^{\sqrt{-1}\omega ih})-(\xi^{n+1}e^{\sqrt{-1}\omega ih})^2\xi^{n+1}e^{-\sqrt{-1}\omega ih}-(\xi^{n+1}e^{\sqrt{-1}\omega ih})^2\xi^n e^{-\sqrt{-1}\omega ih}). \tag{22}$$

This can also be written as

$$\xi^{n+1}e^{\sqrt{-1}\omega ih} = \xi^n e^{\sqrt{-1}\omega ih} - \frac{r}{(\eta-\sqrt{-1}\beta)}(\sum_{j=i-m}^{i} g_j\xi^{n+1}e^{\sqrt{-1}\omega(i-j)h}+(\sum_{j=i-m}^{i} g_j\xi^n e^{\sqrt{-1}\omega(i-j)h})+$$

$$\frac{\tau}{2(\eta-\sqrt{-1}\beta)\varepsilon^2}(V(x)(\xi^{n+1}e^{\sqrt{-1}\omega ih}+\xi^n e^{\sqrt{-1}\omega ih})-(\xi^{n+1}e^{\sqrt{-1}\omega ih})^2\xi^{n+1}e^{-\sqrt{-1}\omega ih}-(\xi^{n+1}e^{\sqrt{-1}\omega ih})^2\xi^n e^{-\sqrt{-1}\omega ih}). \tag{23}$$

where $r = \frac{\tau}{2h^\alpha}$. Let us assume that

$$\Psi_{max}^{(n)} = max[(\Psi_i^n)^2, (\Psi_i^{n+1})^2], \tag{24}$$

which provides us with

$$\xi^{n+1}e^{\sqrt{-1}\omega ih}(1+\frac{r}{(\eta-\sqrt{-1}\beta)}\sum_{j=i-m}^{i} g_j e^{\sqrt{-1}\omega jh}-\frac{\tau}{2(\eta-\sqrt{-1}\beta)}V(x))+\frac{\tau}{2(\eta-\sqrt{-1}\beta)\varepsilon^2}\Psi_{max}^{(n)}\xi^{n+1}e^{\sqrt{-1}\omega ih}$$

$$=\xi^n e^{\sqrt{-1}\omega ih}(1-\frac{r}{(\eta-\sqrt{-1}\beta)}\sum_{j=i-m}^{i} g_j e^{\sqrt{-1}\omega jh}+\frac{\tau}{2(\eta-\sqrt{-1}\beta)}V(x))-\frac{\tau}{2(\eta-\sqrt{-1}\beta)\varepsilon^2}\Psi_{max}^{(n)}\xi^n e^{-\sqrt{-1}\omega ih}. \tag{25}$$

Then by taking the absolute of both the sides of Eq. (25), we get

$$|\xi^{n+1}e^{\sqrt{-1}\omega ih}(1+\frac{r}{(\eta-\sqrt{-1}\beta)}\sum_{j=i-m}^{i} g_j e^{-\sqrt{-1}\omega jh}-\frac{\tau}{2(\eta-\sqrt{-1}\beta)}V(x))|$$

$$\leq |\xi^n e^{\sqrt{-1}\omega ih}(1-\frac{r}{(\eta-\sqrt{-1}\beta)}\sum_{j=i-m}^{i} g_j e^{\sqrt{-1}\omega jh}+\frac{\tau}{2(\eta-\sqrt{-1}\beta)}V(x))-\frac{\tau}{2(\eta-\sqrt{-1}\beta)\varepsilon^2}\Psi_{max}^{(n)}\xi^n e^{-\sqrt{-1}\omega ih}|.$$

$$+|\frac{\tau}{2(\eta-\sqrt{-1}\beta)\varepsilon^2}\Psi_{max}^{(n)}\xi^{n+1}e^{\sqrt{-1}\omega ih}|. \tag{26}$$

After eliminating s from Eq. (26) and rearranging the terms, we get

$$|\xi|(|1+\frac{r}{(\eta-\sqrt{-1}\beta)}\sum_{j=i-m}^{i} g_j e^{-\sqrt{-1}\omega jh}-\frac{\tau}{2(\eta-\sqrt{-1}\beta)}V(x))|-|\frac{\tau}{2(\eta-\sqrt{-1}\beta)\varepsilon^2}\Psi_{max}^{(n)}|)$$

$$\leq |(1-\frac{r}{(\eta-\sqrt{-1}\beta)}\sum_{j=i-m}^{i} g_j e^{-\sqrt{-1}\omega jh}+\frac{\tau}{2(\eta-\sqrt{-1}\beta)}V(x))-\frac{\tau}{2(\eta-\sqrt{-1}\beta)\varepsilon^2}\Psi_{max}^{(n)}|. \tag{27}$$

Further the triangle inequality renders that

$$|z_1| - |z_2| \leq |z_1 - z_2|, \tag{28}$$

which implies that

$$|1 + \frac{r}{(\eta - \sqrt{-1}\beta)} \sum_{j=i-m}^{i} g_j e^{-\sqrt{-1}\omega jh} - \frac{\tau}{2(\eta - \sqrt{-1}\beta)} V(x)| - |\frac{\tau}{2(\eta - \sqrt{-1}\beta)\varepsilon^2} \Psi_{max}^{(n)}|$$

$$\leq |1 + \frac{r}{(\eta - \sqrt{-1}\beta)} \sum_{j=i-m}^{i} g_j e^{-\sqrt{-1}\omega jh} - \frac{\tau}{2(\eta - \sqrt{-1}\beta)} V(x)) - \frac{\tau}{2(\eta - \sqrt{-1}\beta)\varepsilon^2} \Psi_{max}^{(n)}|. \tag{29}$$

So by combining Eq. (27) and Eq. (29), we observe that for satisfying both the inequalities we need

$$|\xi| \leq 1. \tag{30}$$

So, it has been shown that the proposed implicit second order finite difference scheme is unconditionally stable for the fractional CGLS equation via the approach of Von Neumann's stability analysis.

5 The proposed spectral method for the CGLS equation with the Riesz fractional derivative

An effective numerical scheme has been developed in this section for dealing with the following Riesz fractional Complex Ginzburg-Landau-Schrödinger equation

$$(\eta - i\beta)\frac{\partial \psi(x,t)}{\partial t} = -(-\triangle)^{\alpha/2}\psi(x,t) + \frac{1}{\varepsilon^2}(V(x) - |\psi(x,t)|^2)\psi(x,t), \quad x \in \Re, \quad t > 0, \tag{31}$$

with initial condition

$$\psi(x,0) = \mu(x), \quad x \in \Re, \tag{32}$$

where $\psi(x,t)$ is the complex valued wave function.

5.1 *Discretisation procedure*

The mesh size is $h = \frac{b-a}{m}$, m denoting an even integer and $x_j = a + jh$ is taken as the grid points where $j = 0, 1, \cdots, m$. Similarly taking temporal step size τ , the time steps taken as $t_n = n\tau, \quad \tau > 0, n = 0, 1, 2, 3, \cdots$.

5.2 *Methodology*

The first Schrödinger–like equation is tackled in two steps, rather splitting from $t = t_n$ to t_{n+1}. So Eq.(31) has been split in the following way by first solving

$$(\eta - i\beta)\frac{\partial \psi(x,t)}{\partial t} = -(-\triangle)^{\alpha/2}\psi(x,t), \tag{33}$$

and then solving

$$(\eta - i\beta)\frac{\partial \psi(x,t)}{\partial t} = \frac{1}{\varepsilon^2}(V(x) - |\psi(x,t)|^2)\psi(x,t), \tag{34}$$

by taking time step τ in both the equations.
So by applying the TSFS approach for discretizing Eq. (33) in spatial variable, along with applying an integration to Eq. (34) in temporal variable by taking integrating limits from $t = t_n$ to t_{n+1}, we obtain

$$\psi(x,t_{n+1}) = exp[\int_{t_n}^{t_{n+1}} (\frac{1}{\varepsilon^2(\eta - i\beta)})(V(x) - \psi(x,s)\overline{\psi}(x,s))ds]\psi(x,t_n). \tag{35}$$

Further taking a numerical approach via the trapezoidal formula for the purpose of approximation of the integral on $[t_n, t_{n+1}]$ provides us with the solution

$$\psi(x,t_{n+1}) = exp[\frac{1}{2\varepsilon^2(\eta - i\beta)}\tau(2V(x) - (\psi(x,t_{n+1})\overline{\psi}(x,t_{n+1}) + (\psi(x,t_n)\overline{\psi}(x,t_n))]\psi(x,t_n). \tag{36}$$

Now applying the Fourier transform technique to the equation

$$(\eta - i\beta)\frac{\partial \psi(x,t)}{\partial t} = -(-\triangle)^{\alpha/2}\psi(x,t), \tag{37}$$

and further integrating it from $t = t_n$ to t_{n+1}, we obtain

$$\widehat{\psi}(\mu_k, t_{n+1}) = exp(-\frac{1}{\eta - i\beta}|\mu_k|^\alpha \tau)\widehat{\psi}(\mu_k, t_n), \tag{38}$$

where μ_k is the transform parameter taken as $\mu_k = \frac{2\pi k}{b-a}$. Taking the inverse discrete Fourier transform of Eq. (38), we obtain the simplified solution as

$$\psi_j^{**} = \frac{1}{m}\sum_{k=-\frac{m}{2}}^{\frac{m}{2}-1} exp(-\frac{1}{\eta - i\beta}|\mu_k|^\alpha \tau)(\widehat{\psi}^*)_k exp(i\mu_k(x_j - a)), \tag{39}$$

where $(\widehat{\psi}^*)_k$ is the Fourier transform of ψ_j^* defined by

$$(\widehat{\psi}^*)_k(t) = F_k[\psi_j^*(t)] = \sum_{j=0}^{m-1}\psi_j^* exp(-i\mu_k(x_j - a)), \ k = -\frac{m}{2}, \cdots \frac{m}{2} - 1 \tag{40}$$

5.3 Basic idea of the methodology of the splitting scheme via Strang splitting technique

If an ordinary differential equation can be written as

$$f^{'} = L_1(f) + L_2(f), \tag{41}$$

where the exact solutions of $f^{'} = L_1(f)$, denoted by $\phi_t^{L_1}(f(0))$ and $f^{'} = L_2(f)$, denoted by $\phi_t^{L_2}(f(0))$ can be efficiently computed, the splitting techniques often provide an effective alternative in comparison with the traditional integration methods. Moreover the splitting schemes preserve a given property of the ordinary differential equation which is done by the flow generated by L_1 and L_2. Now if the exact partial flows are utilized for a step size τ, then the Strang splitting scheme can be manifested as

$$S_\tau = \phi_{\tau/2}^{L_1} \circ \phi_\tau^{L_2} \circ \phi_{\tau/2}^{L_1}, \tag{42}$$

which is a symmetric technique of second order.
The second order scheme can be otherwise implemented in the following steps

$$\widehat{f_1} = e^{L_1\frac{\tau}{2}}y_0, \overrightarrow{f_1} = e^{L_2\tau}\widehat{f_1}, f_1 = e^{L_1\frac{\tau}{2}}\overrightarrow{f_1} \tag{43}$$

$$\widehat{f_2} = e^{L_1\frac{\tau}{2}}f_1, \overrightarrow{f_2} = e^{L_2\tau}\widehat{f_2}, f_2 = e^{L_1\frac{\tau}{2}}\overrightarrow{f_2}, \tag{44}$$

$$\widehat{f_3} = e^{L_1\frac{\tau}{2}}f_2, \overrightarrow{f_3} = e^{L_2\tau}\widehat{f_3}, f_3 = e^{L_1\frac{\tau}{2}}\overrightarrow{f_3}, \tag{45}$$

$$\vdots$$

$$\widehat{f_n} = e^{L_1\frac{\tau}{2}}f_{n-1}, \overrightarrow{f_n} = e^{L_2\tau}\widehat{f_n}, y_n = e^{L_1\frac{\tau}{2}}\overrightarrow{f_n}, \tag{46}$$

5.4 Implementation of the Strang splitting (SP) scheme for the proposed Riesz fractional CGLS equation

The second order Strang splitting scheme is displayed by the following equations:

$$\psi_j^* = exp[\frac{(\eta+i\beta)}{2\varepsilon^2(\eta^2+\beta^2)}\tau(2V(x)-(\psi(x,t_{n+1})\overline{\psi}(x,t_{n+1})+(\psi(x,t_n)\overline{\psi}(x,t_n))]\psi(x,t_n), \quad j=0,1,2,\cdots,m-1, \tag{47}$$

$$\psi_j^{**} = \frac{1}{m}\sum_{k=-\frac{m}{2}}^{\frac{m}{2}-1} exp(-\frac{1}{\eta-i\beta}|\mu_k|^\alpha\tau)(\widehat{\psi}^*)_k exp(i\mu_k(x_j-a)), \quad j=0,1,2,\cdots,m-1, \tag{48}$$

$$\psi_j^{n+1} = exp[\frac{(\eta+i\beta)}{2\varepsilon^2(\eta^2+\beta^2)}\tau(2V(x)-(\psi(x,t_{n+1})\overline{\psi}(x,t_{n+1})+(\psi(x,t_n)\overline{\psi}(x,t_n))]\psi_j^{**}, \quad j=0,1,2,\cdots,m-1, \tag{49}$$

where $(\widehat{\psi}^*)_k$ is the Fourier transform of ψ_j^* as the definition in Eq. (12).

6 Stability analysis for the proposed spectral scheme for the CGLS equation involving Riesz fractional derivative

Theorem 6.1 The second-order time-splitting scheme Eq. (47), Eq. (48) and Eq. (49) for the Riesz fractional Ginzburg-Landau-Schrödinger equation is unconditionally stable.

Furthermore, the conservative properties are shown as

$$||\Psi^{n+1}||_{l_2}^2 = ||\psi^0||_{l_2}^2, \quad n=0,1,2,\cdots$$

Proof. The L^2- norm and l^2-norm are defined as

$$||\Psi||_{L^2} = \sqrt{\int_a^b|\psi(x)|^2dx}, \ ||\Psi||_{l^2} = \sqrt{\tfrac{b-a}{m}\textstyle\sum_{j=0}^{m-1}|\psi_j|^2}.$$

By using Eq. (39), Eq. (13) and Eq. (6) for the schemes in Eq. (47), Eq. (48) and Eq. (49), we have

$$\tfrac{1}{b-a}||\Psi^{n+1}||_{l_2}^2 = \tfrac{1}{m}\textstyle\sum_{j=0}^{m-1}|\psi_j^{n+1}|^2$$

$$= \frac{1}{m}\sum_{j=0}^{m-1}|exp[\frac{(\eta+i\beta)}{2\varepsilon^2(\eta^2+\beta^2)}\tau(2V(x)-(\psi(x,t_{n+1})\overline{\psi}(x,t_{n+1})+(\psi(x,t_n)\overline{\psi}(x,t_n))]\psi_j^{**}|^2 \quad = \frac{1}{m}\sum_{j=0}^{m-1}|\psi_j^{**}|^2$$

$$= \frac{1}{m}\sum_{j=0}^{m-1}|\frac{1}{m}\sum_{k=-\frac{m}{2}}^{\frac{m}{2}-1} exp(-\frac{\eta+i\beta}{\eta^2+\beta^2}|\mu_k|^\alpha\tau)(\widehat{\psi}^*)_k exp(i\mu_k(x_j-a))|^2 = \frac{1}{m^2}\sum_{k=-\frac{m}{2}}^{\frac{m}{2}-1}|exp(-\frac{\eta+i\beta}{\eta^2+\beta^2}|\mu_k|^\alpha\tau)(\widehat{\psi}^*)_k|^2$$

$$= \frac{1}{m^2}\sum_{k=-\frac{m}{2}}^{\frac{m}{2}-1}|(\widehat{\psi}^*)_k|^2 = \frac{1}{m^2}\sum_{k=-\frac{m}{2}}^{\frac{m}{2}-1}|\sum_{j=0}^{m-1}\psi_j^* exp(-i\mu_k(x_j-a))|^2 = \frac{1}{m}\sum_{j=0}^{m-1}|\psi_j^*|^2$$

$$= \frac{1}{m}\sum_{j=0}^{m-1}|\psi_j^n|^2 = \frac{1}{b-a}||\Psi^n||_{l_2}^2. \tag{50}$$

Furthermore the identities used here are

$$\sum_{j=0}^{m-1} exp(i2\pi(l-k)j/M) = \begin{cases} 0, & l-k\neq mM \\ M, & l-k=mM \ , \ Misaninteger \end{cases}. \tag{51}$$

and

$$\sum_{j=0}^{m-1} exp(i2\pi(l-j)k/M) = \begin{cases} 0, & l-j\neq mM \\ M, & l-j=mM \ , \ Misaninteger \end{cases}. \tag{52}$$

Therefore, the result in Eq. (6) can be obtained from Eq. (50) for the splitting scheme ((47))- ((49)) by the method of mathematical induction.

7 Numerical discussion

Example 1: Here the CGLS equation ((31)) has been considered with the following initial condition

$$\psi_0(x) = \sqrt{1 - (\frac{20\pi}{L})^2} exp(i\frac{20\pi}{L}x). \quad (53)$$

Here $L = 100$ and the constants in Eq. (31) are taken as $\eta = 1$ and $\beta = 1$ respectively. Here the interval for x is taken as $[-5,5]$. Also the value for $\varepsilon = 1$ and the constant in external potential $V(x)$ is taken as $\gamma_x = 1$ which gives $V(x) = \frac{1}{1+exp(-x^2)}$.

This section includes the numerical discussion and representation of the results obtained by the time splitting Fourier spectral method for the CGLS Eq. (31) and Eq. (32). In this context, Table 1 contains the comparison for the values of $|\psi(x,t)|^2$, $Re(\psi(x,t))$ and $Im(\psi(x,t))$ obtained by the TSFS scheme and IFDM, providing the absolute errors for Example 1 for $-5 \leq x \leq 5$ and $t = 0.5$. . Further here the spatial step size $h = 0.2$ and temporal step size $\tau = 0.1$ are considered taking two cases for $\alpha = 1.5$ and $\alpha = 1.75$. Apart from that the error norms L^2- norm and $L^\infty-$ norm for the absolute values, real values and imaginary values for the complex wave function $\psi(x,t)$ have been displayed in Table 2 for various values of x and t taking $\alpha = 1.5$ and $\alpha = 1.75$.

Table 1: Absolute errors for fractional Complex Ginzburg-Landau-Schrödinger (CGLS) Eq. (31) obtained by using TSFS approximation and IFDM solutions for Example 1 at various points of x and $t = 0.5$ taking temporal step size $\tau = 0.1$ with $\alpha = 1.5$ and $\alpha = 1.75$.

x	$\alpha = 1.5(Ex\ 1)$ $t = 0.5$	$\alpha = 1.75(Ex\ 1)$ $t = 0.5$	$\alpha = 1.5(Ex\ 1)$ $t = 0.5$	$\alpha = 1.75(Ex\ 1)$ $t = 0.5$	$\alpha = 1.5(Ex\ 1)$ $t = 0.5$	$\alpha = 1.75(Ex\ 1)$ $t = 0.5$
x	Absolute errors between $\vert\psi\vert^2_{TSFS}$ and $\vert\psi\vert^2_{IFDM}$	Absolute errors between $\vert\psi\vert^2_{TSFS}$ and $\vert\psi\vert^2_{IFDM}$	Absolute errors between $Re(\psi)_{TSFS}$ and $Re(\psi)_{IFDM}$	Absolute errors between $Re(\psi)_{TSFS}$ and $Re(\psi)_{IFDM}$	Absolute errors between $Im(\psi)_{TSFS}$ and $Im(\psi)_{IFDM}$	Absolute errors between $Im(\psi)_{TSFS}$ and $Im(\psi)_{IFDM}$
-4.8	1.0033E-4	1.2083E-4	3.2087E-3	1.4736E-2	5.6849E-2	8.1894E-2
-4.0	1.0056E-5	2.5915E-7	1.4175E-2	8.1883E-2	2.16643E-2	3.0983E-3
-3.4	3.3765E-7	3.7743E-5	3.1259E-2	9.6138E-2	5.9323E-3	5.0476E-2
-2.8	3.4743E-5	3.9741E-5	2.5270E-2	2.4288E-3	4.7090E-2	6.7967E-3
-2.0	1.3558E-4	2.6029E-4	2.8179E-3	1.0852E-2	6.2378E-2	7.0617E-2
-1.2	3.4166E-4	2.5277E-4	7.6303E-3	2.617E-2	6.1600E-2	3.5265E-2
-0.4	5.7204E-5	5.4308E-4	2.9220E-2	8.7249E-3	6.15342E-3	1.7022E-2
0.4	2.68671E-4	5.6204E-5	7.2001E-3	9.7932E-3	3.4291E-2	4.3205E-3
1.2	1.5544E-4	1.3548E-4	1.1562E-2	1.5159E-2	3.1303E-2	3.5453E-3
2.0	3.30865E-4	2.018E-4	5.3281E-3	2.1847E-3	5.5893E-2	7.5154E-2
2.8	5.1080E-4	9.2081E-6	7.2196E-4	2.3859E-2	4.5733E-2	7.0903E-3
3.4	1.53906E-4	1.45906E-4	2.2517E-3	7.5222E-4	4.4443E-3	6.2556E-3
4.0	3.20545E-6	1.8843E-7	1.0017E-3	1.9566E-3	8.1083E-3	5.9469E-2
4.8	2.65729E-6	2.6095E-7	9.443E-3	7.028E-3	1.7045E-2	7.6215E-3

Table 2: L^2 norm and L^∞ norm of errors between the solutions of TSFS method and IFDM for Example 1 at $t = 0.5$ and 1, for $\alpha = 1.5$ and $\alpha = 1.75$.

x	Ex 1 $\alpha = 1.5$	Ex 1 $\alpha = 1.5$	Ex 1 $\alpha = 1.5$	Ex 1 $\alpha = 1.5$	Ex 1 $\alpha = 1.5$	Ex 1 $\alpha = 1.5$
	L^2 error of $\vert\psi(x,t)\vert^2$	L^∞ error of $\vert\psi(x,t)\vert^2$	L^2 error of $Re(\psi(x,t))$	L^∞ error of $Re(\psi(x,t))$	L^2 error of $Im(\psi(x,t))$	L^∞ error of $Im(\psi(x,t))$
0.5	3.8237E-4	2.9388E-2	1.8793E-2	4.166E-2	4.735E-2	8.3122E-2
1.0	1.8071E-2	3.2506E-2	3.5968E-2	2.1704E-1	9.7688E-2	7.072E-2

x	Ex 1 $\alpha = 1.75$	Ex 1 $\alpha = 1.75$	Ex 1 $\alpha = 1.75$	Ex 1 $\alpha = 1.75$	Ex 1 $\alpha = 1.75$	Ex 1 $\alpha = 1.75$
	L^2 error of $\lvert\psi(x,t)\rvert^2$	L^∞ error of $\lvert\psi(x,t)\rvert^2$	L^2 error of $Re(\psi(x,t))$	L^∞ error of $Re(\psi(x,t))$	L^2 error of $Im(\psi(x,t))$	L^∞ error of $Im(\psi(x,t))$
0.5	9.36681E-4	5.555E-3	1.80006E-2	4.0034E-2	4.794E-2	7.272E-4
1.0	2.7596E-3	3.9618E-3	2.149E-2	8.501E-2	3.5003E-2	7.7483E-2

Here for a fixed time t_l , the L^∞ norm for error is defined as

$$L^\infty \equiv Max_{-m\le i\le m}|\psi_{IFDM}(x_i,t_l)-\psi_{TSFS}(x_i,t_l)| \tag{54}$$

and further L^2 norm for error is formulated as

$$L^2 \equiv \sqrt{\frac{1}{2m+1}\sum_{i=1}^{2m+1}(\psi_{IFDM}(x_i,t_l)-\psi_{TSFS}(x_i,t_l))^2}. \tag{55}$$

Apart from the tabulated results, the solutions from the proposed techniques have been manifested by depicting the 2D as well as 3D plots for $|\psi(x,t)|^2$, $Re(\psi(x,t))$ and $Im(\psi(x,t))$ by taking fractional order $\alpha = 1.5$ and $\alpha = 1.75$. separately, for various values of x in $[-5,5]$ and at $t = 0.5$. Apart from that, comparison of graphs obtained by both TSFS and IFDM have been depicted here for $|\psi(x,t)|^2$, $Re(\psi(x,t))$ and $Im(\psi(x,t))$ by taking fractional order $\alpha = 1.5$ and $\alpha = 1.75$.

In Fig. 1, Fig. 2, Fig. 3, Fig. 4, Fig. 5 and Fig. 6 the graphical 2D solutions for $|\psi(x,t)|^2$, $Re(\psi(x,t))$ and $Im(\psi(x,t))$ are depicted for Example 1 for the both cases i.e. taking $\alpha = 1.5$ and $\alpha = 1.75$. separately. Further the corresponding 3D figures obtained by TSFS method for $|\psi(x,t)|^2$, $Re(\psi(x,t))$ and $Im(\psi(x,t))$ for Example 1 are shown in Fig. 7, Fig. 8, Fig. 9, Fig. 10, Fig. 11 and Fig. 12 respectively. Moreover the graphs obtained by the comparison of TSFS technique and IFDM are displayed in Fig. 13 and Fig. 14 for $|\psi(x,t)|^2$, , in Fig. 15 and Fig.16 for $Re(\psi(x,t))$ and $Im(\psi(x,t))$ in Fig. 17 and Fig. 18 by taking fractional orders $\alpha = 1.5$ and $\alpha = 1.75$ separately.

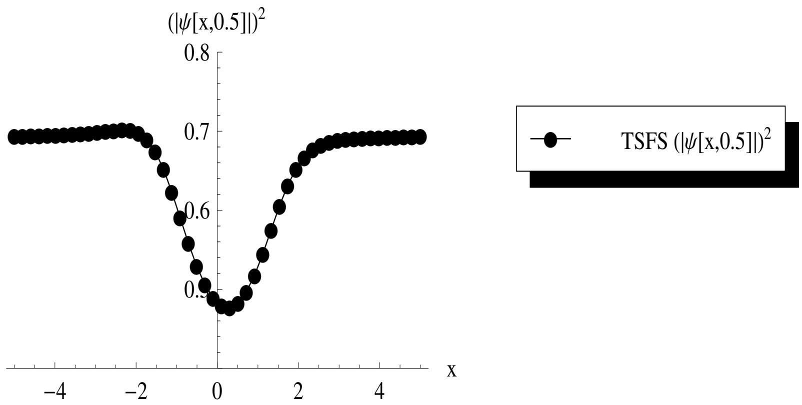

Fig. 1: Graphical 2D solutions for $|\psi(x,t)|^2$ of Example 1 via TSFS for the fractional CGLS equation for $\alpha = 1.5$

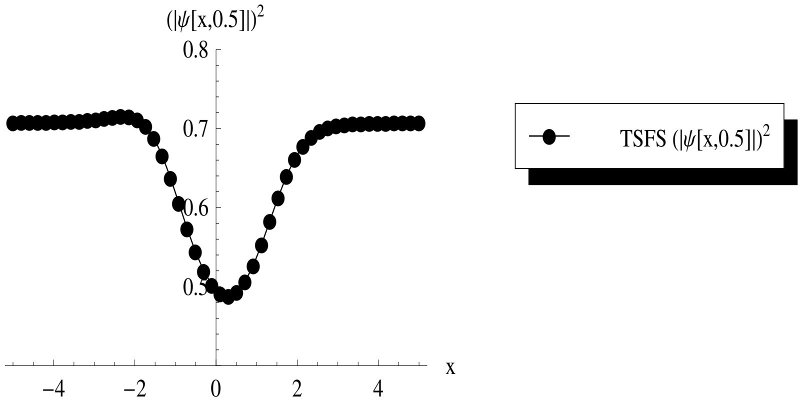

Fig. 2: Graphical 2D solutions for $|\psi(x,t)|^2$ of Example 1 via TSFS for the fractional CGLS equation for $\alpha = 1.75$

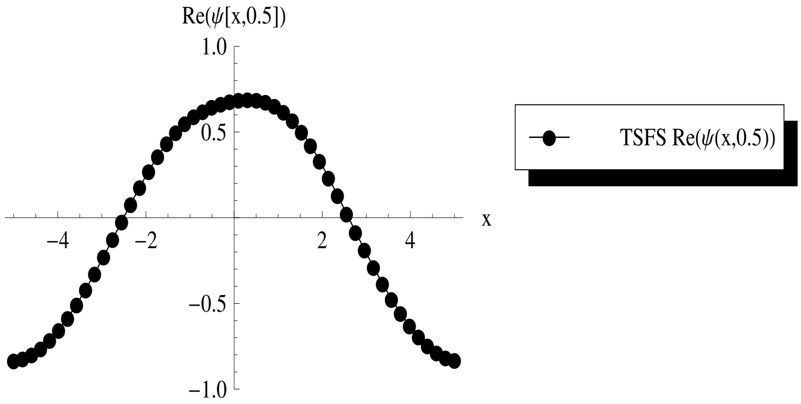

Fig. 3: Graphical 2D solutions for $Re(\psi(x,t))$ of Example 1 via TSFS for the fractional CGLS equation for $\alpha = 1.5$

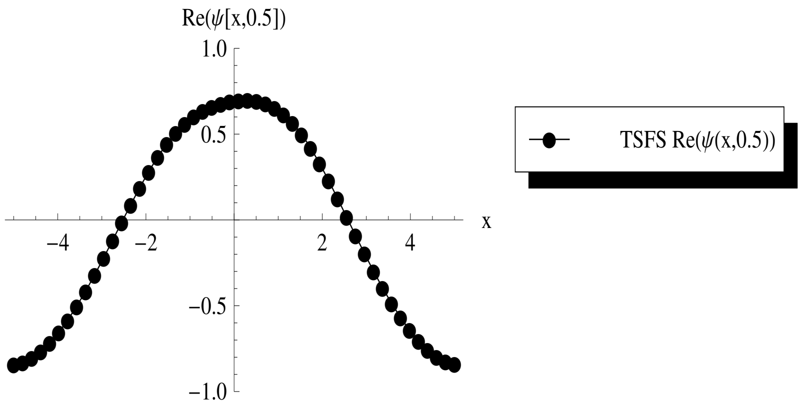

Fig. 4: Graphical 2D solutions for $Re(\psi(x,t))$ of Example 1 via TSFS for the fractional CGLS equation for $\alpha = 1.75$

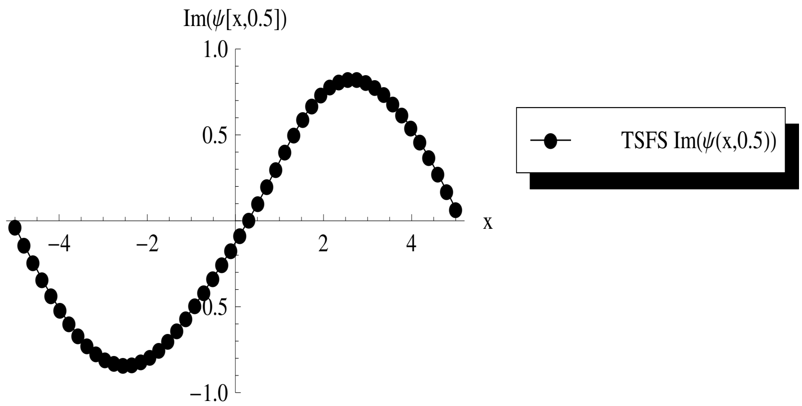

Fig. 5: Graphical 2D solutions for $Im(\psi(x,t))$ of Example 1 via TSFS for the fractional CGLS equation for $\alpha = 1.5$

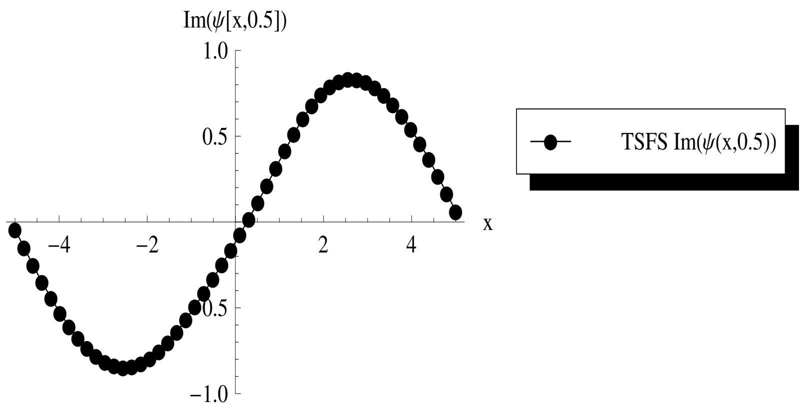

Fig. 6: Graphical 2D solutions for $Im(\psi(x,t))$ of Example 1 via TSFS for the fractional CGLS equation for $\alpha = 1.75$

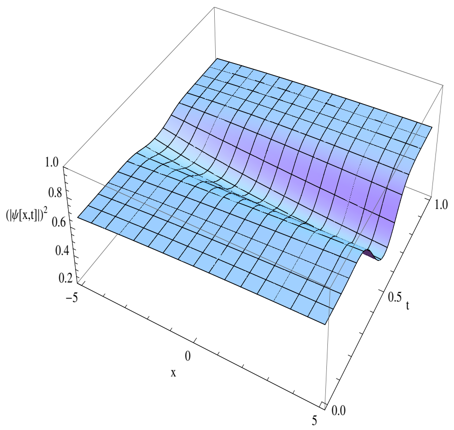

Fig. 7: Graphical 3D solutions for $|\psi(x,t)|^2$ of Example 1 via TSFS for the fractional CGLS equation for $\alpha = 1.5$

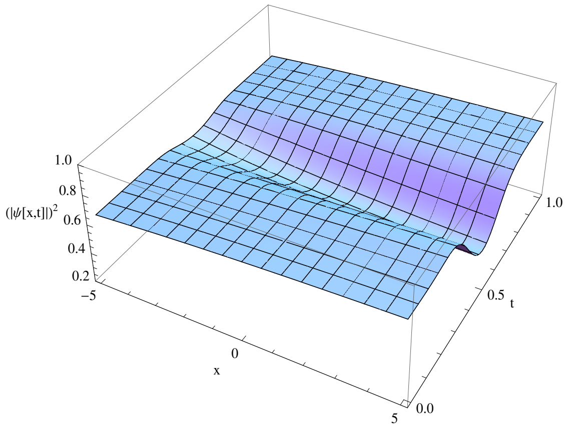

Fig. 8: Graphical 3D solutions for $|\psi(x,t)|^2$ of Example 1 via TSFS for the fractional CGLS equation for $\alpha = 1.75$

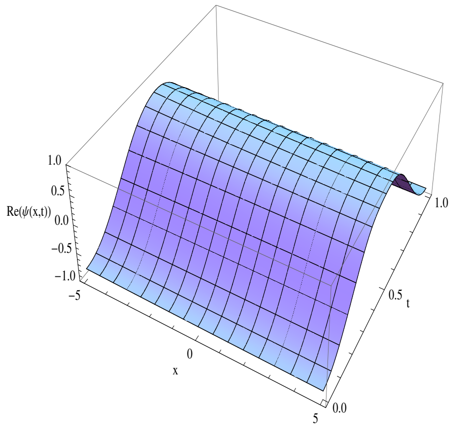

Fig. 9: Graphical TSFS 3D solutions for $Re(\psi(x,t))$ of Example 1 for the fractional CGLS equation for various points of x at $t = 0.5$ with $\alpha = 1.5$

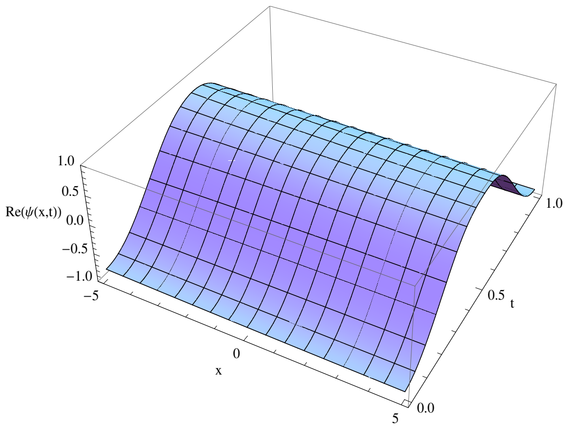

Fig. 10: Graphical 3D solutions for $Re(\psi(x,t))$ of Example 1 via TSFS for the fractional CGLS equation for $\alpha = 1.75$

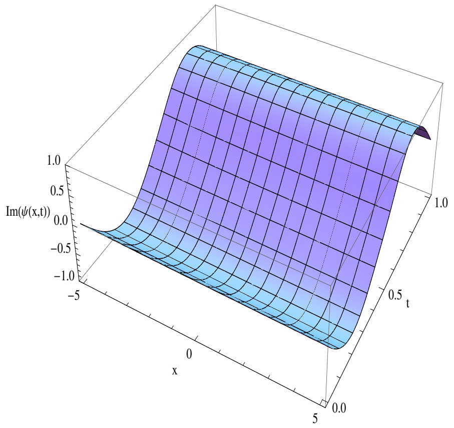

Fig. 11: Graphical 3D solutions for $Im(\psi(x,t))$ of Example 1 via TSFS for the fractional CGLS equation for $\alpha = 1.5$

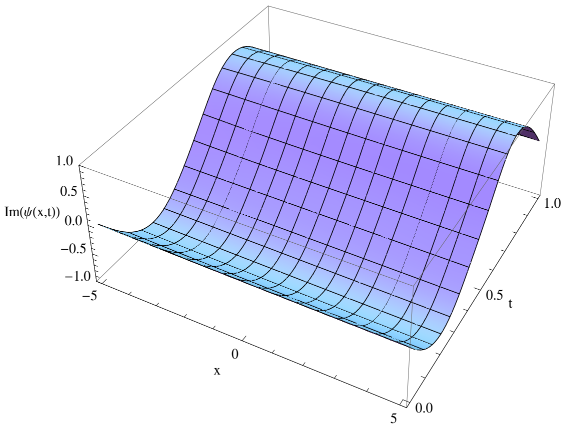

Fig. 12: Graphical 3D solutions for $Im(\psi(x,t))$ of Example 1 via TSFS for the fractional CGLS equation for $\alpha = 1.75$

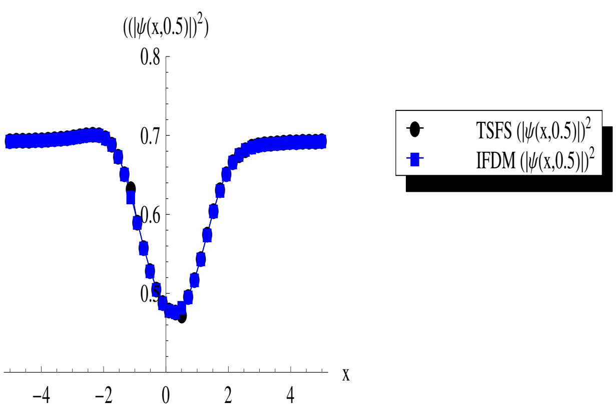

Fig. 13: Graphical comparison of $|\psi(x,t)|^2$ obtained from TSFS method and IFDM for the CGLS Eq. (31) for Example 1 with $\alpha = 1.5$ at $t = 0.5$

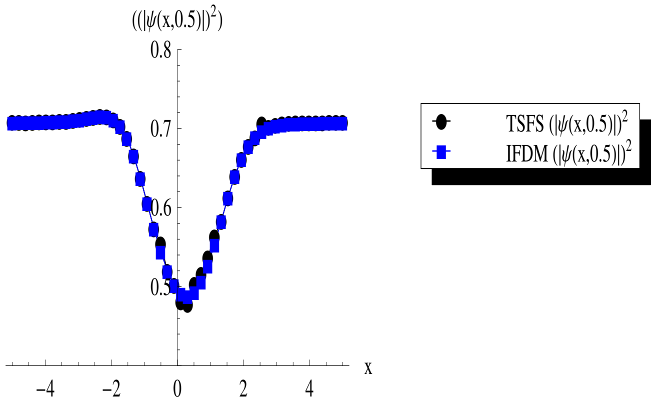

Fig. 14: Graphical comparison of $|\psi(x,t)|^2$ obtained from TSFS method and IFDM for the CGLS Eq. (31) for Example 1 with $\alpha = 1.75$ at $t = 0.5$

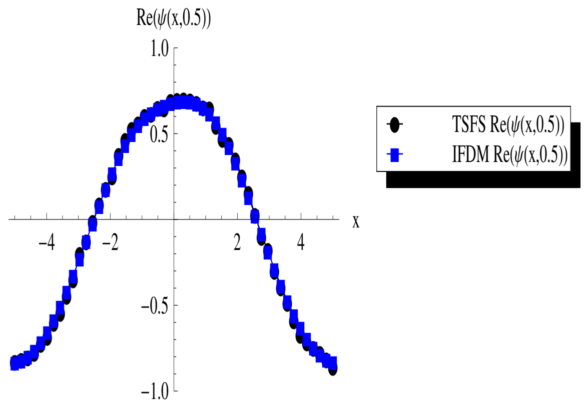

Fig. 15: Graphical comparison of $Re(\psi(x,t))$ obtained from TSFS method and IFDM for the CGLS Eq. (31) for Example 1 with $\alpha = 1.5$ at $t = 0.5$

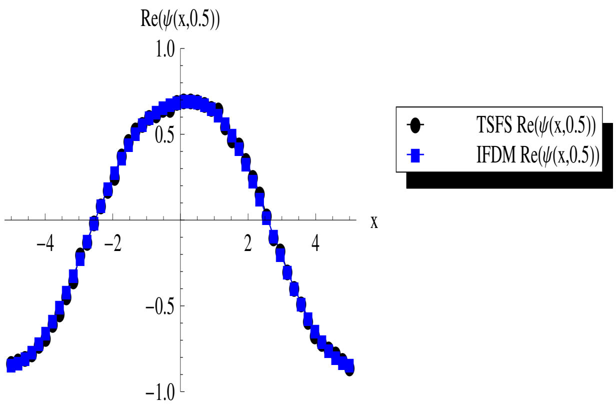

Fig. 16: Graphical comparison of $Re(\psi(x,t))$ obtained from TSFS method and IFDM for the CGLS Eq. (31) for Example 1 with $\alpha = 1.75$ at $t = 0.5$

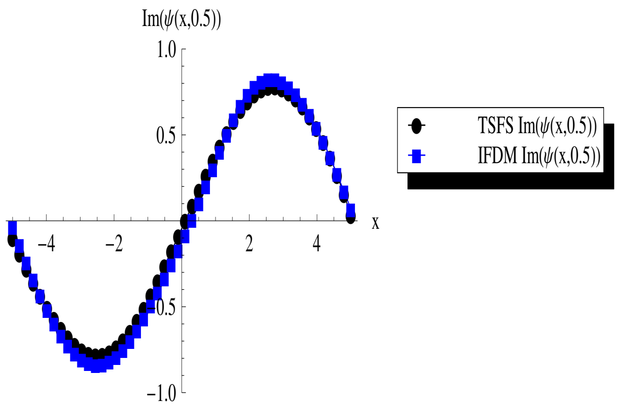

Fig. 17: Graphical comparison of $Im(\psi(x,t))$ obtained from TSFS method and IFDM for the CGLS Eq. (31) for Example 1 with $\alpha = 1.5$ at $t = 0.5$

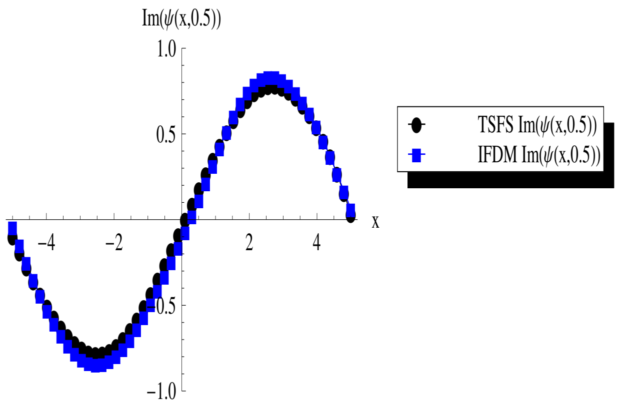

Fig. 18: Graphical comparison of $Im(\psi(x,t))$ obtained from TSFS method and IFDM for the CGLS Eq. (31) for Example 1 with $\alpha = 1.75$ at $t = 0.5$

8 Conclusion

In the present paper the fractional CGLS equation with the Riesz derivative has been tackled via an implicit second-order finite difference method (IFDM), where the fractional centered difference scheme is applied for the approximation of the Riesz fractional derivative. The stability of the implicit scheme has also been represented via von Neumann stability analysis. Further a comparative study has been put forth in the later section via a second order splitting scheme named Strang splitting technique for the investigation of the efficacy and efficiency of the results obtained. Moreover the spectral scheme is proved to be unconditionally stable. The results computed by the methods, for the absolute errors, manifests the existence of a fine tuning between the solutions obtained from both the approaches. Further the solutions of the methods have been used to display the error norms L^2 and L^∞ for $|\psi(x,t)|^2$, $Re(\psi(x,t))$ and $Im(\psi(x,t))$ of Example 1. Furthermore, the results have also been displayed graphically.

Acknowledgement

I am thankful to the authorities of my institute, National Institute of Technology to permit me for successfully carrying out this piece of research work.

References

[1] I. Podlubny, *Fractional differential equations*, Academic Press, New York, 1999.
[2] K. S. Miller and B. Ross, *An introduction to fractional calculus and fractional differential equations*, John Wiley, New York, NY, USA, 1993.
[3] S. G. Samko, A. A. Kilbas and O. I. Marichev, *Fractional integrals and derivatives: theory and applications*, Gordan and Breach, New York, NY, USA, 1993.
[4] R. Hilfer, *Applications of fractional calculus in physics*, World Scientific Press, Singapore, 2000.
[5] W. Bao, S. Jin and P. A. Markowich, On time-splitting spectral approximations for the Schrödinger equations in the semiclassical regime, *J. Comput. Phys.* **175**, 487–584 (2002).
[6] H. Borluk, G. M. Muslu and H. A. Erbay, A numerical study of the long wave-short wave interaction equations, *Math. Comput. Simul.* **74**, 113–25 (2007).
[7] W. Bao and L. Yang, Efficient and accurate numerical methods for the Klein-Gordon- Schrödinger equation, *J. Comput. Phys.* **225**, 1863–93 (2007).
[8] C. Celik and M. Duman, Crank-Nicolson method for the fractional diffusion equation with the Riesz fractional derivative, *J. Comput. Phys.* **231**, 1743–1750 (2012).
[9] F. H. Lin and Q. Du, Ginzburg-Landau vortices: Dynamics, pinning and hysteresis, *SIAM J. Math. Anal.* **28**, 1265–1293 (1997).
[10] Y. Zhang, W. Bao and Q. Du, Numerical simulation of vortex dynamics in Ginzburg-Landau-Schrödinger equation, *Eur. J. Appl. Math.* **18**, 607–630 (2007).
[11] A. Patra, An effective comparison involving a novel spectral approach and the finite difference method for the Schrödinger equation involving the Riesz fractional derivative in the quantum field theory, *Eur. Phys. J. Plus* **133(3)**, 1–14 (2018).
[12] A. A. Aderogba, M. Chapwanya and J. K. Djoko, On a fractional step-splitting scheme for the Cahn-Hilliard equation, *Eng. Comput.* **31(7)**, 1151–1168 (2014).
[13] N. Thapa and M. Gudejko, Numerical solution of heat equation by spectral method, *Appl. Math. Sci.* **8(8))**, 397–404 (2014).
[14] S. Saha Ray, On the time-splitting Fourier spectral method for the coupled Klein- Gordon-Schrödinger equations in the quantum field theory, *Eng. Comput.* **34(7)**, 2344–2357 (2017).
[15] M. Thalhammer, M. Caliari and C. Neuhauser, High-order time-splitting Hermite and Fourier spectral methods, *J Comput. Phys.* **228**, 822–832 (2009).
[16] H. Y. Jian and Y. D. Wang, Ginzburg Landau vortices in inhomogeneous superconductors, *J. Part. Differ. Equ.* **15**, 45–60 (2002).
[17] D. Bai and J. Wang, The time-splitting Fourier spectral method for the coupled Schrödinger-Boussinesq equations, *Commun. Nonlin. Sci.* **17**, 1201–1210 (2012).
[18] P. A. Markowich, P. Pietra and C. Pohl, Numerical approximation of quadratic observables of Schrödinger-type equations in the semi-classical limit, *Numer. Math.* **81(4)**, 595–630 (1999).
[19] H. Wang, A time-splitting spectral method for the coupled Gross-Pitaevskii equations with applications to rotating Bose-Einstein condensates, *J Comput. Phys.* **205**, 88–104 (2007).